Erratum: Standard Model predictions for $B \to K\ell^+\ell^-$, $B \to K\ell_1^-\ell_2^+$ and $B \to K\nu\bar{\nu}$ using form factors from $N_f = 2+1+1$ lattice QCD [Phys. Rev. D 107, 014511 (2023)]

W. G. Parrott, C. Bouchard, and C. T. H. Davies

(HPQCD Collaboration)

(Received 7 April 2023; published 14 June 2023)

DOI: 10.1103/PhysRevD.107.119903

In our analysis of the phenomenology of $B \to K\ell^+\ell^-$ we normalized our differential rate using $\alpha_{\rm EW}$ at the scale M_Z when the consideration of electroweak corrections implies that a better scale would be $\mu = m_b$ [1]. We also mistakenly included an additional factor of $\eta_{\rm EW}$. Equation (3) of Sec. II for the normalization factor should read

$$\begin{aligned} \mathcal{C} &= \frac{G_F^2 \alpha_{\rm EW}^2 |V_{tb} V_{ts}^*|^2}{2^9 \pi^5 M_B^3} \beta_\ell \sqrt{\lambda(q, M_B, M_K)}, \\ \beta_\ell &= \sqrt{1 - 4m_\ell^2/q^2}, \\ \lambda(a,b,c) &= a^4 + b^4 + c^4 - 2(a^2b^2 + a^2c^2 + b^2c^2). \end{aligned} \tag{3}$$

We take the value of $1/\alpha_{\rm EW} = 132.32(5)$ at the scale $\mu = 4.2$ GeV and this number should replace the value given in Table 1. It is obtained by running down from $1/\alpha_{\rm EW} = 132.14(4)$ at $\mu = 4.8$ GeV [2]. We use this latter value when accounting for the systematic error from the dependence of our results on μ. This change affects our discussion of the differential and total branching fractions for $B \to K\ell^+\ell^-$. It does not affect our results for the ratio of branching fractions to different leptons in the final state, or to our discussion of the flat term, F_H^ℓ.

Figures 3, 4 and 5 plot our updated differential branching fractions as blue bands for the cases of positively charged mesons, neutral mesons, and the average of the two, respectively, across the full physical q^2 range. They are compared to experimental results for decays to electrons, muons or both (averaged) shown for each experimental q^2 bin. As before, our results are somewhat higher than experiment in most cases, particularly in the region $4 \le q^2/\text{GeV}^2 \le 8.68$. This is most clearly visible in Fig. 3, where the tension between our result and the most precise data from LHCb is obvious.

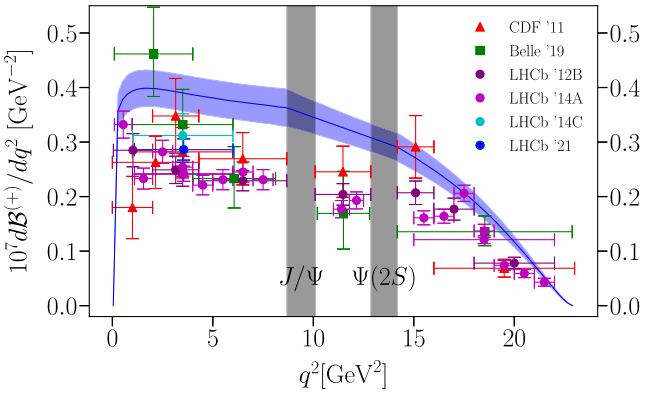

FIG. 3. Differential branching fraction for $B^+ \to K^+\ell^+\ell^-$, with our result in blue, compared with experimental results. Note that Belle '19, and LHCb '14C and '21 have $\ell = e$, while otherwise $\ell = \mu$. Horizontal error bars indicate bin widths.

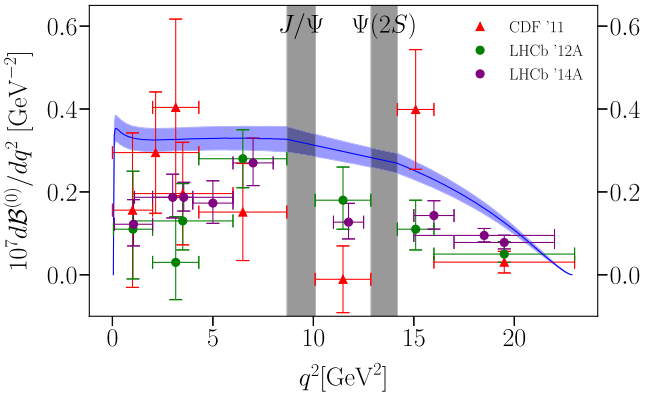

FIG. 4. Differential branching fraction for $B^0 \to K^0\ell^+\ell^-$, with our result in blue, compared with experimental results. All experimental results take $\ell = \mu$. Horizontal error bars indicate bin widths.

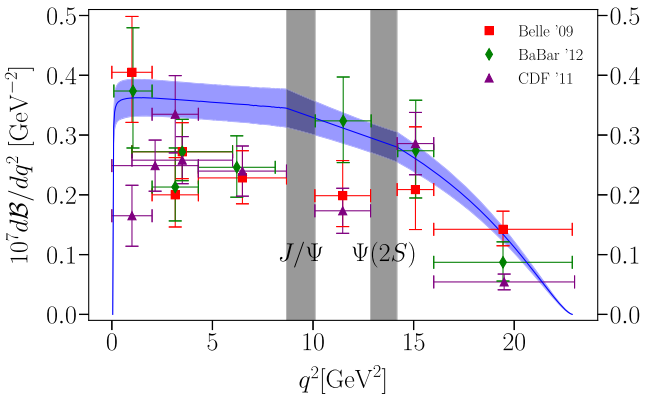

FIG. 5. Differential branching fraction for $B \to K\ell^+\ell^-$, with our result in blue, compared with experimental results. CDF '11 takes $\ell = \mu$, whilst Belle '09 and Babar '12 do not differentiate e from μ. Horizontal error bars indicate bin widths.

TABLE III. Comparison of branching fractions with recent experimental results in well-behaved regions of q^2. Note that the $B^+ \to K^+e^+e^-$ result quoted here from LHCb '21 is obtained using the $B^+ \to K^+\mu^+\mu^-$ result from LHCb '14A, combined with the ratio determined in LHCb '21. In the fifth column, the tension is given by mean(Experiment–HPQCD)/σ(Experiment–HPQCD).

Channel	Result	q^2/GeV^2 range	$\mathcal{B} \times 10^7$	Tension with HPQCD '22
$B^+ \to K^+e^+e^-$	LHCb '21	(1.1, 6)	$1.401^{+0.074}_{-0.069} \pm 0.064$	-2.7σ (-2.4σ)
$B^+ \to K^+e^+e^-$	HPQCD '22	(1.1, 6)	$1.91 \pm 0.16(\pm 0.095)_{\text{QED}}$	...
$B^+ \to K^+e^+e^-$	Belle '19	(1, 6)	$1.66^{+0.32}_{-0.29} \pm 0.04$	-0.8σ (-0.8σ)
$B^+ \to K^+e^+e^-$	HPQCD '22	(1, 6)	$1.94 \pm 0.16(\pm 0.097)_{\text{QED}}$	...
$B^0 \to K^0\mu^+\mu^-$	LHCb '14A	(1.1, 6)	$0.92^{+0.17}_{-0.15} \pm 0.044$	-3.1σ (-3.1σ)
$B^0 \to K^0\mu^+\mu^-$	HPQCD '22	(1.1, 6)	$1.60 \pm 0.14(\pm 0.032)_{\text{QED}}$	...
$B^0 \to K^0\mu^+\mu^-$	LHCb '14A	(15, 22)	$0.67^{+0.11}_{-0.11} \pm 0.035$	-2.7σ (-2.7σ)
$B^0 \to K^0\mu^+\mu^-$	HPQCD '22	(15, 22)	$1.070 \pm 0.095(\pm 0.021)_{\text{QED}}$	...
$B^+ \to K^+\mu^+\mu^-$	Belle '19	(1, 6)	$2.30^{+0.41}_{-0.38} \pm 0.05$	$+0.8\sigma$ $(+0.8\sigma)$
$B^+ \to K^+\mu^+\mu^-$	HPQCD '22	(1, 6)	$1.95 \pm 0.16(\pm 0.039)_{\text{QED}}$	...
$B^+ \to K^+\mu^+\mu^-$	LHCb '14A	(1.1, 6)	$1.186 \pm 0.034 \pm 0.059$	-4.2σ (-4.1σ)
$B^+ \to K^+\mu^+\mu^-$	HPQCD '22	(1.1, 6)	$1.91 \pm 0.16(\pm 0.038)_{\text{QED}}$	...
$B^+ \to K^+\mu^+\mu^-$	LHCb '14A	(15, 22)	$0.847 \pm 0.028 \pm 0.042$	-2.8σ (-2.7σ)
$B^+ \to K^+\mu^+\mu^-$	HPQCD '22	(15, 22)	$1.16 \pm 0.10(\pm 0.023)_{\text{QED}}$	...

We give the updated Table III comparing our branching fractions integrated over well-behaved q^2 regions with experiment. We find our partial branching fractions to be significantly higher than the experimental values, typically with tensions exceeding 2.7σ. The tension reaches 4.1σ for LHCb'14A in the low q^2 region for $B^+ \to K^+\mu^+\mu^-$. These results are illustrated in Fig. 6.

Figures 7, 8 and 9 give our updated total branching fractions, again in comparison to experiment. We see clear tension with LHCb'14A of 3.9σ for $B^+ \to K^+\mu^+\mu^-$ and 4.2σ for $B^0 \to K^0\mu^+\mu^-$. Our updated value for the total branching fraction to τ leptons in the final state is $\mathcal{B}_\tau^{(+)} = 1.68(12) \times 10^{-7}$.

The comparison to other theoretical results for $B \to K\ell^+\ell^-$ is not qualitatively changed and we do not update those figures here.

Our results for $B \to K\ell_1^-\ell_2^+$ change in line with those for $B \to K\ell^+\ell^-$ because the functions $\phi_i(q^2)$ use the same normalization. We give the updated Table IV of results for the integrals over the $\phi_i(q^2)$ denoted a_K^{12}, b_K^{12}, e_K^{12} and f_K^{12} below. We also give the updated Figs. 27, 28 and 29 for the functions $\phi_i(q^2)$.

Our results for the differential rates and total branching fraction for the rare decay $B \to K\nu\bar{\nu}$ are not affected by the issues discussed above because there we used an electroweak correction factor X_t appropriate to the choice of parameters $\alpha_{\rm EW}(M_Z)$ and $\sin^2\theta_W(M_Z)$. However we mistakenly introduced a factor $\eta_{\rm EW}$ and we correct for that here. Equation (15) should read

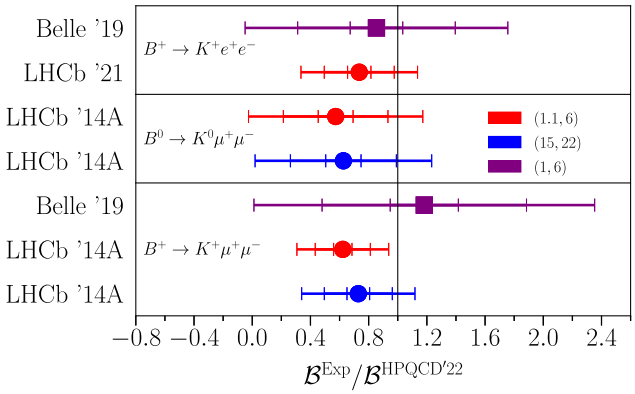

FIG. 6. Comparison of branching fractions with recent experimental results in well behaved regions of q^2. Here we show the ratio of the experimental branching fraction to our results, meaning our results correspond to the line at 1. The error bars are 5σ long, with markers at 1, 3 and 5σ. Note that the σ here are different from those calculated in Table III. On the right, labels indicate q^2 bins in units of GeV^2.

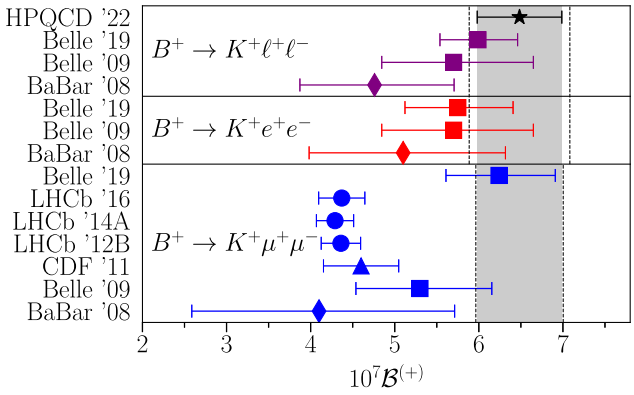

FIG. 7. The total branching fraction for $B^+ \to K^+\ell^+\ell^-$. Our result (HPQCD '22) is given by the black band, as compared with experimental results. Dashed lines indicate the effect of adding QED uncertainty to our result.

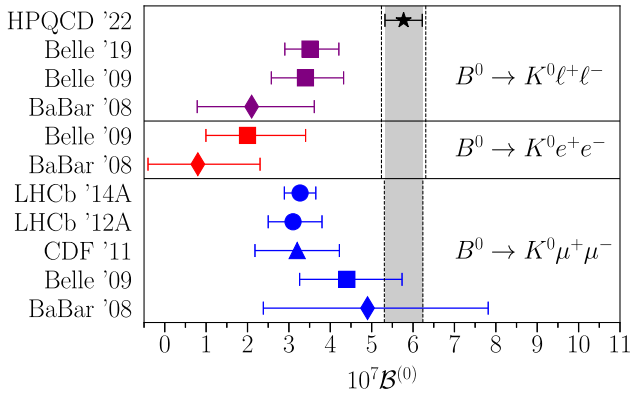

FIG. 8. The total branching fraction for $B^0 \to K^0\ell^+\ell^-$. Our result (HPQCD '22) is given by the black band, as compared with experimental results. Dashed lines indicate the effect of adding QED uncertainty to our result.

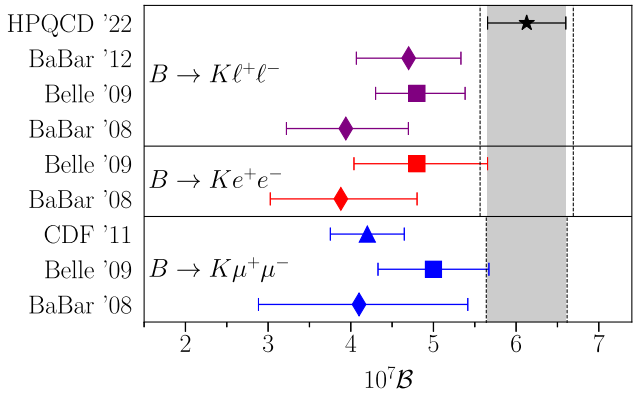

FIG. 9. The total branching fraction for $B \to K\ell^+\ell^-$. Our result (HPQCD '22) is given by the black band, as compared with experimental results. Dashed lines indicate the effect of adding QED uncertainty to our result.

$$\frac{d\mathcal{B}(B \to K\nu\bar{\nu})_{\rm SD}}{dq^2} = \frac{G_F^2\alpha_{\rm EW}^2(M_Z)X_t^2}{32\pi^5\sin^4\theta_W}\tau_B|V_{tb}V_{ts}^*|^2|\vec{p}_K|^3 f_+^2(q^2). \tag{15}$$

Since $\eta_{\rm EW}$ was very close to 1, there is no visible difference in any plots, but our updated values for the branching fractions that appear in Table V are

TABLE IV. Results for the coefficients of Eqs. (10) and (11) for $B^0 \to K^0\ell_1\ell_2$ and $B^+ \to K^+\ell_1\ell_2$ decay. No additional uncertainty is included for QED effects.

$\ell_1\ell_2$	a_K^{12}	b_K^{12}	e_K^{12}	f_K^{12}
$B^0 \to K^0 e\mu$	17.7(1.2)	17.7(1.2)	24.5(1.4)	24.5(1.4)
$B^0 \to K^0 e\tau$	11.08(69)	11.08(69)	13.97(79)	13.97(79)
$B^0 \to K^0\mu\tau$	10.85(69)	11.26(69)	13.44(76)	14.41(82)
$B^+ \to K^+ e\mu$	19.2(1.3)	19.2(1.3)	26.6(1.5)	26.6(1.5)
$B^+ \to K^+ e\tau$	11.99(75)	11.99(75)	15.14(86)	15.15(86)
$B^+ \to K^+\mu\tau$	11.73(75)	12.18(75)	14.57(83)	15.62(89)

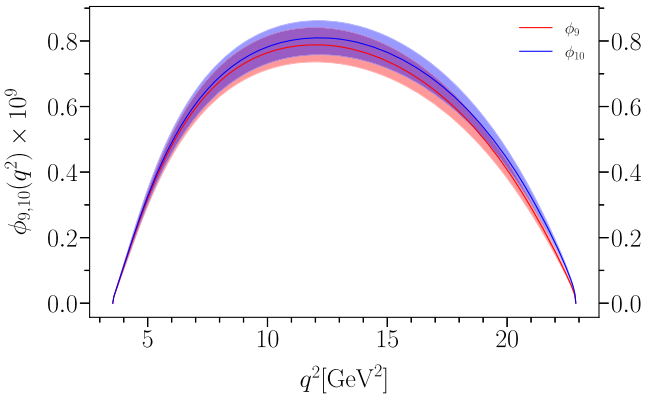

FIG. 27. $\phi_{9,10}(q^2) \times 10^9$ for the $B^0 \to K^0 \mu\tau$ decay.

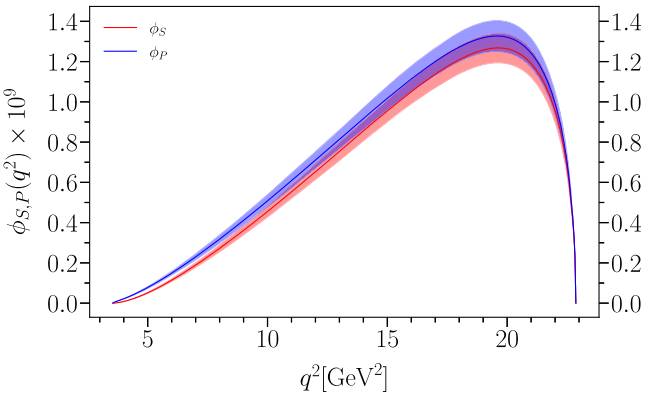

FIG. 28. $\phi_{S,P}(q^2) \times 10^9$ for the $B^0 \to K^0 \mu\tau$ decay.

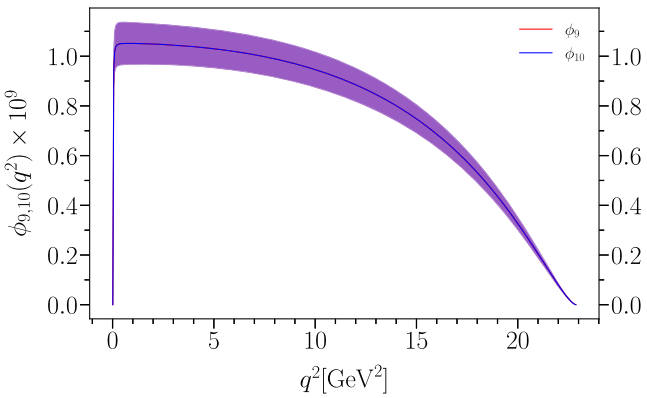

FIG. 29. $\phi_{9,10}(q^2) \times 10^9$ for the $B^0 \to K^0 e\mu$ decay.

$$\mathcal{B}(B^0 \to K^0 \nu\bar{\nu}) = 4.60(34) \times 10^{-6},$$
$$\mathcal{B}(B^+ \to K^+ \nu\bar{\nu}) = 5.58(37) \times 10^{-6},$$

where the charged meson case includes the long-distance component given in Eq. (16).

We thank Sébastien Descotes-Genon and Quim Matias for pointing out the issue with the scale of α_{EW}.

APPENDIX: NUMERICAL RESULTS

Here we update the numerical values that change in Tables VI, VII and X of Appendix C.

TABLE VI. Short distance contributions to branching fractions $\mathcal{B}^{(0/+)} = \mathcal{B}(B^{0/+} \to K^{0/+}\nu\bar{\nu})_{\rm SD}$ (Equation (15) for the rare decay $B \to K\nu\bar{\nu}$ integrated over various q^2 bins. Numerical values for q^2 bins are in units of GeV^2.

q^2 bin	(0.001, 4)	(4, 8)	(8, 12)	(12, 16)	(16, 20)	$(20, q^2_{\rm max})$
$10^6\mathcal{B}(B^+ \to K^+\nu\bar{\nu}_{\rm SD})$	1.173(95)	1.139(89)	1.056(83)	0.892(71)	0.589(47)	0.125(11)
$10^6\mathcal{B}(B^0 \to K^0\nu\bar{\nu}_{\rm SD})$	1.087(88)	1.056(82)	0.979(77)	0.826(65)	0.543(43)	0.1133(96)

TABLE VII. Branching fractions integrated over some commonly used q^2 binning schemes for the electron, muon and ℓ, which is the average of the two. In the first bin of the top panel, giving the branching fraction integrated over the full q^2 range, the first number is the whole integral, whilst the one which follows in square brackets is the result when the ranges 8.68–10.11 GeV^2 and 12.86–14.18 GeV^2 are excluded. Numerical values for q^2 bins are in units of GeV^2. QED corrections are not included here.

q^2 bin	$(4m^2_\ell, q^2_{\rm max})$	(0.05, 2)	(1, 6)	(2, 4.3)	(4.3, 8.68)	(14.18, 16)	(16, 18)	(18, 22)
$10^7\mathcal{B}(B^+ \to K^+e^+e^-)$	6.50(50) [5.59(43)]	0.752(65)	1.94(16)	0.902(76)	1.63(15)	0.491(44)	0.441(39)	0.458(41)
$10^7\mathcal{B}(B^0 \to K^0e^+e^-)$	5.79(45) [4.97(39)]	0.655(57)	1.64(14)	0.751(64)	1.44(13)	0.454(41)	0.407(36)	0.419(38)
$10^7\mathcal{B}(B \to Ke^+e^-)$	6.14(48) [5.28(41)]	0.703(61)	1.79(15)	0.826(69)	1.54(13)	0.473(42)	0.424(38)	0.438(40)
$10^7\mathcal{B}(B^+ \to K^+\mu^+\mu^-)$	6.48(50) [5.59(43)]	0.746(64)	1.95(16)	0.902(75)	1.63(15)	0.492(44)	0.442(39)	0.459(41)
$10^7\mathcal{B}(B^0 \to K^0\mu^+\mu^-)$	5.77(45) [4.95(38)]	0.648(57)	1.64(14)	0.751(64)	1.44(13)	0.455(41)	0.408(36)	0.421(38)
$10^7\mathcal{B}(B \to K\mu^+\mu^-)$	6.13(47) [5.27(40)]	0.697(60)	1.79(15)	0.827(69)	1.54(13)	0.473(42)	0.425(38)	0.440(40)
$10^7\mathcal{B}(B^+ \to K^+\ell^+\ell^-)$	6.49(50) [5.59(43)]	0.749(65)	1.94(16)	0.902(76)	1.63(15)	0.492(44)	0.442(39)	0.458(41)
$10^7\mathcal{B}(B^0 \to K^0\ell^+\ell^-)$	5.78(45) [4.96(39)]	0.652(57)	1.64(14)	0.751(64)	1.44(13)	0.455(41)	0.408(36)	0.420(38)
$10^7\mathcal{B}(B \to K\ell^+\ell^-)$	6.14(47) [5.27(40)]	0.700(60)	1.79(15)	0.827(69)	1.54(13)	0.473(42)	0.425(38)	0.439(40)

q^2 bin	(0.1, 2)	(2, 4)	(4, 6)	(6, 8)	(15, 17)	(17, 19)	(19, 22)	(1.1, 6)	(15, 22)
$10^7\mathcal{B}(B^+ \to K^+e^+e^-)$	0.736(64)	0.786(66)	0.761(66)	0.740(66)	0.495(44)	0.380(34)	0.284(26)	1.91(16)	1.16(10)
$10^7\mathcal{B}(B^0 \to K^0e^+e^-)$	0.636(55)	0.653(56)	0.658(57)	0.658(58)	0.458(41)	0.350(31)	0.259(24)	1.60(14)	1.067(95)
$10^7\mathcal{B}(B \to Ke^+e^-)$	0.686(59)	0.719(60)	0.709(59)	0.699(61)	0.477(42)	0.365(33)	0.271(25)	1.75(15)	1.113(99)
$10^7\mathcal{B}(B^+ \to K^+\mu^+\mu^-)$	0.733(63)	0.786(66)	0.762(66)	0.741(66)	0.496(44)	0.381(34)	0.285(26)	1.91(16)	1.16(10)
$10^7\mathcal{B}(B^0 \to K^0\mu^+\mu^-)$	0.633(55)	0.653(56)	0.658(57)	0.658(58)	0.459(41)	0.351(31)	0.260(24)	1.60(14)	1.070(95)
$10^7\mathcal{B}(B \to K\mu^+\mu^-)$	0.683(59)	0.720(60)	0.710(59)	0.700(61)	0.477(42)	0.366(33)	0.273(25)	1.76(15)	1.116(99)
$10^7\mathcal{B}(B^+ \to K^+\ell^+\ell^-)$	0.734(63)	0.786(66)	0.761(66)	0.741(66)	0.496(44)	0.380(34)	0.285(26)	1.91(16)	1.16(10)
$10^7\mathcal{B}(B^0 \to K^0\ell^+\ell^-)$	0.635(55)	0.653(56)	0.658(57)	0.658(58)	0.458(41)	0.351(31)	0.260(24)	1.60(14)	1.068(95)
$10^7\mathcal{B}(B \to K\ell^+\ell^-)$	0.685(59)	0.719(60)	0.710(59)	0.699(61)	0.477(42)	0.365(33)	0.272(25)	1.76(15)	1.114(99)

q^2 bin	(0.1, 4)	(4, 8.12)	(10.2, 12.8)	$(14.18, q^2_{\rm max})$	(10.09, 12.86)	$(16, q^2_{\rm max})$
$10^7\mathcal{B}(B^+ \to K^+e^+e^-)$	1.52(13)	1.55(14)	0.847(70)	1.40(12)	0.903(75)	0.910(81)
$10^7\mathcal{B}(B^0 \to K^0e^+e^-)$	1.29(11)	1.35(12)	0.772(64)	1.29(11)	0.823(68)	0.836(75)
$10^7\mathcal{B}(B \to Ke^+e^-)$	1.41(12)	1.45(12)	0.809(67)	1.35(12)	0.863(71)	0.873(78)
$10^7\mathcal{B}(B^+ \to K^+\mu^+\mu^-)$	1.52(13)	1.55(14)	0.847(70)	1.40(12)	0.904(75)	0.913(81)
$10^7\mathcal{B}(B^0 \to K^0\mu^+\mu^-)$	1.29(11)	1.36(12)	0.773(64)	1.29(11)	0.824(68)	0.838(75)
$10^7\mathcal{B}(B \to K\mu^+\mu^-)$	1.40(12)	1.45(12)	0.810(67)	1.35(12)	0.864(71)	0.876(78)
$10^7\mathcal{B}(B^+ \to K^+\ell^+\ell^-)$	1.52(13)	1.55(14)	0.847(70)	1.40(12)	0.903(75)	0.911(81)
$10^7\mathcal{B}(B^0 \to K^0\ell^+\ell^-)$	1.29(11)	1.36(12)	0.773(64)	1.29(11)	0.824(68)	0.837(75)
$10^7\mathcal{B}(B \to K\ell^+\ell^-)$	1.40(12)	1.45(12)	0.810(67)	1.35(12)	0.864(71)	0.874(78)

TABLE X. Branching fractions for decays to τ leptons, integrated over some commonly used q^2 bins. Numerical values for q^2 bins are in units of GeV^2. No uncertainty to allow for QED is included in these numbers.

q^2 bin	$(4m_\tau^2, q^2_{\mathrm{max}})$	$(14.18, q^2_{\mathrm{max}})$	(14.18, 16)	(16, 18)	(18, 22)	(15, 17)	(17, 19)	(19, 22)	(15, 22)
$10^7\mathcal{B}(B^+ \to K^+\tau^+\tau^-)$	1.68(12)	1.49(10)	0.358(26)	0.426(30)	0.656(46)	0.419(30)	0.414(29)	0.454(32)	1.288(90)
$10^7\mathcal{B}(B^0 \to K^0\tau^+\tau^-)$	1.55(11)	1.375(95)	0.332(24)	0.394(28)	0.604(42)	0.388(28)	0.383(27)	0.417(29)	1.188(83)
$10^7\mathcal{B}(B \to K\tau^+\tau^-)$	1.62(11)	1.43(10)	0.345(25)	0.410(29)	0.630(44)	0.403(29)	0.399(28)	0.436(30)	1.238(86)

[1] Christoph Bobeth, Paolo Gambino, Martin Gorbahn, and Ulrich Haisch, Complete NNLO QCD analysis of $\bar{B} \to X_s\ell^+\ell^-$ and higher order electroweak effects, J. High Energy Phys. 04 (2004) 071.

[2] A. A. Pivovarov, Running electromagnetic coupling constant: Low-energy normalization and the value at M(Z), Phys. At. Nucl. **65**, 1319 (2002).